

# Hierarchical ZnO films with microplate/nanohole structures induced by precursor concentration and colloidal templates, their superhydrophobicity, and enhanced photocatalytic performance

Zhigang Li

*Department of Physics & Electronic Engineering, Taizhou University, Taizhou, Zhejiang 318000, China*

Guotao Duan, Guangqiang Liu, and Zhengfei Dai

*Key Laboratory of Materials Physics and School of Materials Science and Engineering, Institute of Solid State Physics, Anhui Key Laboratory of Nanomaterials and Nanotechnology, Chinese Academy of Sciences, Hefei 230031, Anhui, China*

Jinlian Hu

*School of Materials Science and Engineering, Anhui University of Technology, Ma-An-Shan 243002, Anhui, China*

Weiping Cai and Yue Li<sup>a)</sup>

*Key Laboratory of Materials Physics and School of Materials Science and Engineering, Institute of Solid State Physics, Anhui Key Laboratory of Nanomaterials and Nanotechnology, Chinese Academy of Sciences, Hefei 230031, Anhui, China*

(Received 24 March 2013; accepted 31 May 2013)

A facile inexpensive route has been developed to prepare ZnO hierarchical materials with microplate/nanohole structures based on the colloidal monolayer template by the precursor thermal decomposition. These hierarchical structured materials demonstrated an excellent superhydrophobicity with self-cleaning effect and an enhanced photocatalytic performance to organic molecules, which are attributed to big roughness and large surface area of such special hierarchical structures. The formation mechanism of such hierarchical structures was investigated in detail by tracing morphology changing at different precursor concentrations. At high precursor concentration, both incompletely restricted ZnO growth of colloidal templates and preferable growth of microplates take place at the same time, and hence, ZnO hierarchical materials with microplate/nanohole structures are formed. With increasing precursor concentration, the number density of ZnO microplates tends to be larger. The large number density of ZnO microplates and holes on the microplates render the sample a large surface area and surface roughness, leading to good superhydrophobicity and photocatalytic activity. Such hierarchical ZnO micro/nanostructured materials have important applications in environmental science, microfluidic devices, etc.

## I. INTRODUCTION

Nanomaterials have been recently widely studied due to their many applications in different fields, for instance, microelectric and photonic devices,<sup>1</sup> biotechnology,<sup>2,3</sup> piezotronic devices,<sup>4</sup> and catalysts<sup>5</sup> for several decades. However, some nanomaterials, particularly for nanoparticles, have fatal flaws of unstable dispersion in the solution. They will be aggregated together in a long storing time in the liquid media, obstructing their practical applications. Hierarchical micro/nanostructures, complex microstructures composed of micro- and nanostructures, can not only overcome some disadvantages of pure nanosized materials but also offer the advantages of both microsized structures and nanostructures and hence have many applications in microfluidic devices, optoelectronic devices, biomedical

science, surface science, field emission, etc.<sup>6–10</sup> In general, hierarchical structures could be created by the replication induced by an electric field,<sup>6</sup> electron irradiation,<sup>11</sup> solvent thermal route,<sup>12,13</sup> replication routes,<sup>14,15</sup> etc.

Superhydrophobic surfaces [water contact angle (CA) large than 150°] with self-cleaning effect have recently received much attention owing to their applications in preventing the adhesion of water or snow to desired surfaces, antioxidation coating, and microfluidic devices.<sup>16–22</sup> Superhydrophobicity is generally induced by low free energy chemical composition and enough roughness on the material surfaces, which is revealed by investigation of morphologies and components of lotus leaves (lotus effect) that eliminates dirt and contamination on their surfaces.<sup>16</sup> Lotus effect discovers that self-cleaning phenomenon might be realized by superhydrophobicity of a surface with a water CA larger than 150° and a sliding angle (SA) less than 10°.<sup>17</sup> Inspired by this, different methods to prepare superhydrophobic surfaces have been developed,<sup>17–22</sup>

<sup>a)</sup>Address all correspondence to this author.

e-mail: yueli@issp.ac.cn

DOI: 10.1557/jmr.2013.182

including a rough polymer surface by plasma etching,<sup>23</sup> a hierarchical micro/nanostructured film by the wet chemical method,<sup>24</sup> rough films by chemical vapor deposition,<sup>25</sup> binary colloidal structures by self-assembly,<sup>26</sup> a transparent boehmite/silica film by sublimation,<sup>27</sup> superhydrophobic rough surfaces by electrochemical methods,<sup>28</sup> polymer patterns by the polymerization on the etched silicon substrate,<sup>29</sup> stable bionic superhydrophobic surfaces by solution-immersion process,<sup>30</sup> and porous films by electron irradiation or template techniques.<sup>31–33</sup> One of the important approaches is the colloidal template technique to create superhydrophobic surfaces. Colloidal monolayer is usually used as a flexible template to fabricate periodic nanostructured arrays including nanoparticle, nanopore, nanowire, and nanotube arrays.<sup>32–36</sup> It is composed of regularly packed colloidal spheres and belongs to a type of rough surface, which is very useful to design superhydrophobic films using it as a substrate or a template. For example, periodic patterns based on colloidal monolayer templates including pore arrays,<sup>37–39</sup> hierarchical micro/nano PS/CNT or PS/Ag nanoparticle composite arrays,<sup>40,41</sup> nanopillar arrays,<sup>42</sup> etc. exhibited very excellent superhydrophobicity. However, those routes have disadvantages of high costs or complicated experimental operation. Additionally, lotus effect also unveils that hierarchical micro/nanostructures are propitious to realize the superhydrophobicity with self-cleaning effect. Therefore, it is crucial to develop hierarchical micro/nanostructures with self-cleaning effect by a facile inexpensive method.

In this work, we develop a simple route with low cost to prepare hierarchical ZnO microplate/nanohole structured materials based on the colloidal monolayer template by the precursor thermal decomposition. These hierarchical structured materials demonstrated an excellent superhydrophobicity with self-cleaning effect. Additionally, it also displayed enhanced photocatalytic performance to organic molecules. The superhydrophobicity and enhanced photocatalytic property of ZnO hierarchical micro/nanostructured materials are attributed to big roughness and large surface area of such special hierarchical structures. The formation mechanism of such hierarchical structures was investigated in detail by tracing morphology changing at different precursor concentrations. Such hierarchical ZnO micro/nanostructured materials have important applications in environmental science, microfluidic devices, etc.

## II. EXPERIMENTAL

A colloidal suspension with 350-nm monodispersed polystyrene (PS) spheres of 2.5 wt% was purchased from the Alfa Aesar Co. (Ward Hill, MA). First, a colloidal monolayer with PS spheres was prepared on cleaned glass substrates by self-assembly at the interface between air and water and subsequent formation on the substrate after

complete evaporation of the water, as Giersig et al.<sup>43</sup> described. A droplet of 0.5 M zinc nitrate solution was then added on the substrate with a colloidal monolayer template and the solution would infiltrate into the space between colloidal template and substrate through interstices among PS spheres. After drying at room temperature, the template-containing precursor was heated at 100 °C for 1 h and finally annealed at 400 °C for 3 h. The hierarchical ZnO microplate/nanohole structured materials were thus prepared.

To reduce the surface energy on such hierarchical micro/nanostructures, the as-prepared samples were modified with fluoroalkylsilane by a chemical route. The samples were immersed in an ethanol solution of 10 mM 1H, 1H, 2H, 2H-perfluorodecyltrichlorosilane ( $(\text{CF}_3(\text{CF}_2)_7(\text{CH}_2)_2\text{SiCl}_3$ , Alfa Aesar Co.) for 60 min, followed by washing the samples in ethanol to remove the redundant fluoroalkylsilane. The samples were finally dried in an oven at 110 °C for 30 min, introducing a thin layer of perfluorosilane on the sample surfaces. Static water CAs were measured on a G10 (KRÜSS GmbH, Berlin, Germany) at room temperature. The weight of individual water droplets used for the static CA measurements was 2 mg. CA values were achieved by averaging five measurement results on different areas of the sample surface. The SA was measured as follows: a droplet of 2 mg water was added on the sample surface, and it began to slide down when the sample was tilted. The angle at which the sample was tilted was recorded as the SA.

Photocatalytic characterization of such ZnO hierarchical micro/nanostructures was carried out as follows. The as-prepared samples were immersed in a 20 mM stearic acid ethanol solution for 15 h and then taken out and dried at room temperature. The stearic acid molecules were adsorbed onto the sample surface. The samples with stearic acid layer were then irradiated with UV light at ambient atmosphere. A SLUV-6 light source supplied the UV light with a wave length of 254 nm and a power of 90 W (or light intensity of 1.27 W/cm<sup>2</sup>). The degradation of stearic acid under UV illumination was monitored by measuring the decay of the infrared peaks for the symmetric and asymmetric vibrations of CH<sub>2</sub> by a Fourier transform infrared spectroscopy (FTIR) spectrometer (JASCO FT-IR 420) in a diffuse reflectance mode.

The morphology of the as-prepared sample was characterized with a field emission-scanning electron microscope (FE-SEM, Sirion 200, FEI Company, Hillsboro, OR). The x-ray diffraction (XRD) measurement was performed to identify the crystal structure of the as-prepared sample on a Philips X'Pert instrument (The Hague, Netherlands) with Cu K<sub>α</sub> radiation. The x-ray photoelectron spectra (XPS) were characterized by an Escalabmk2 spectrophotometer (Vg Corporation, London, UK) at a take-off angle of 45° relative to the surface normal for the different silver surfaces.

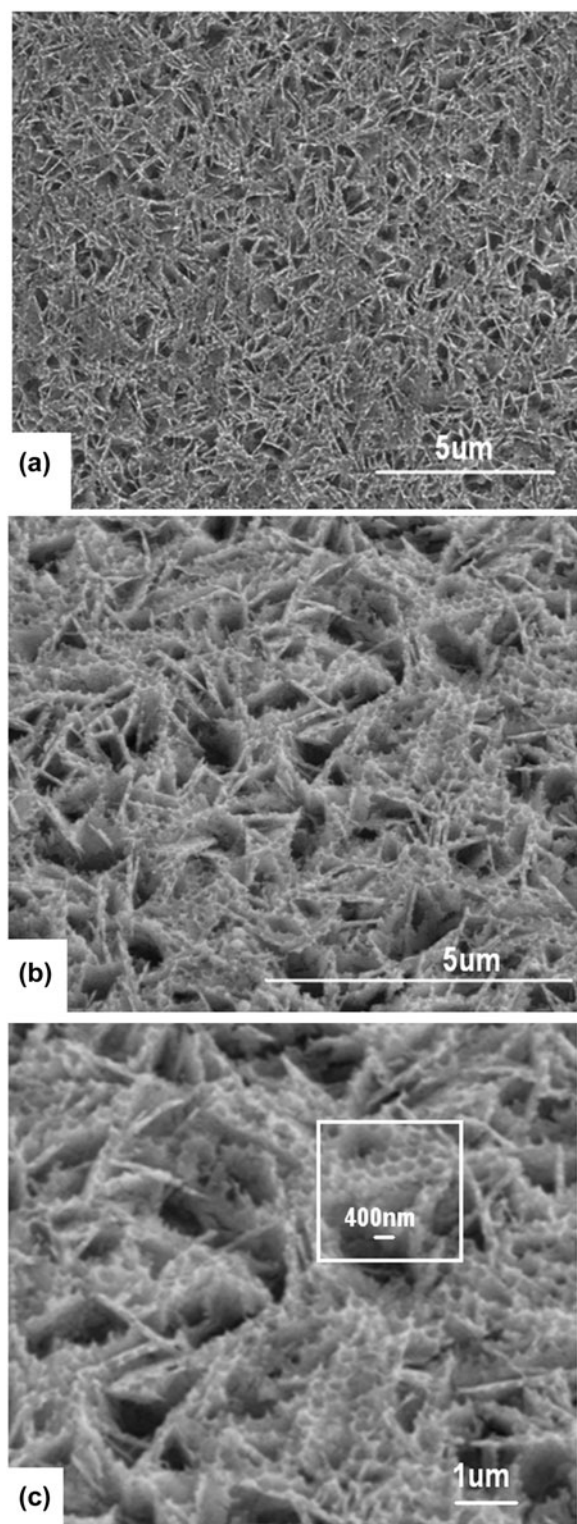


FIG. 1. FE-SEM images of the as-prepared sample obtained using a PS colloidal monolayer as a template by precursor thermal decomposition (PS sphere size: 350 nm). (a) and (b) FE-SEM images observed from top and at tilted angle of 45°, respectively. (c) High magnification of figure b, white frame: highlight of nanohole arrays on the plate surface.

### III. RESULTS AND DISCUSSION

Figure 1 presents the FE-SEM images of a sample obtained using a colloidal monolayer with a PS sphere size of 350 nm as a template and 0.7 M zinc nitrate as a precursor after drying and then annealing. From the top view of the sample, one can find that some microsized plates are formed on the sample and there are some nanoholes on the microplates, as shown in Fig. 1(a). From the image observed with tilted angle [Fig. 1(b)], one can clearly see that microplates uniformly distributed on the substrate with random orientation and their size ranged from 1 to 3  $\mu\text{m}$ . The nanoholes on the microplate exhibited hexagonal arrangement and their sizes are uniform and similar to the PS sphere size, which templated from a colloidal monolayer.

The XPS spectra indicate that the as-prepared sample is composed of the elements of zinc, oxygen, and carbon (Fig. 2). Zn and O should originate from hierarchical micro/nanostructured films and the atomic ratio of Zn and O was about 1:1, which came from the thermal decomposition of the precursor in the annealing process. Carbon originating from impurities in the air is always detected in XPS measurement. According to the XRD spectrum, all the observed diffraction peaks can be well assigned to ZnO, reflecting that the as-prepared sample consists of crystalline ZnO (Fig. 3). The XPS and XRD results indicate that these hierarchical micro/nanostructured films are crystalline ZnO formed in the annealing process at 400 °C for 3 h by the thermal decomposition of the precursor.

The wettability was characterized for this ZnO hierarchical micro/nanostructured film by measuring the water CA. Before measuring, the sample was placed in a light-shaded chamber with clean air for 1 week. The water droplet on the sample surface is shown in Fig. 4(a) and the corresponding water CA is 138°. However, after the surface chemical modification with fluoroalkylsilane, the water CA of the sample dramatically increased to 168°, and the water droplet on the surface was kept almost spherical [Fig. 4(b)], reflecting that the wettability of the surface was changed to superhydrophobicity due to the chemical treatment. Additionally, the SA is less than 5° after modification with low free energy materials.

The photocatalytic activity of the as-prepared hierarchical ZnO micro/nanostructures was characterized based on the degradation of stearic acid under UV irradiation by monitoring the FTIR spectra.<sup>44,45</sup> The frequencies of 2919 and 2849  $\text{cm}^{-1}$  reflect the methylene group asymmetric ( $\nu_{\text{asymm}}\text{CH}_2$ ) and symmetric ( $\nu_{\text{symm}}\text{CH}_2$ ) stretching modes of stearic acid. These values for the methylene group stretching mode are very close to those of a crystalline alkane and are typically taken as evidence of the formation of a well-ordered, dense, self-assembled monolayer of stearic acid on the ZnO surface.<sup>46</sup> With increase of the UV irradiation time, the vibrational bands of the methylene group gradually decreased and almost

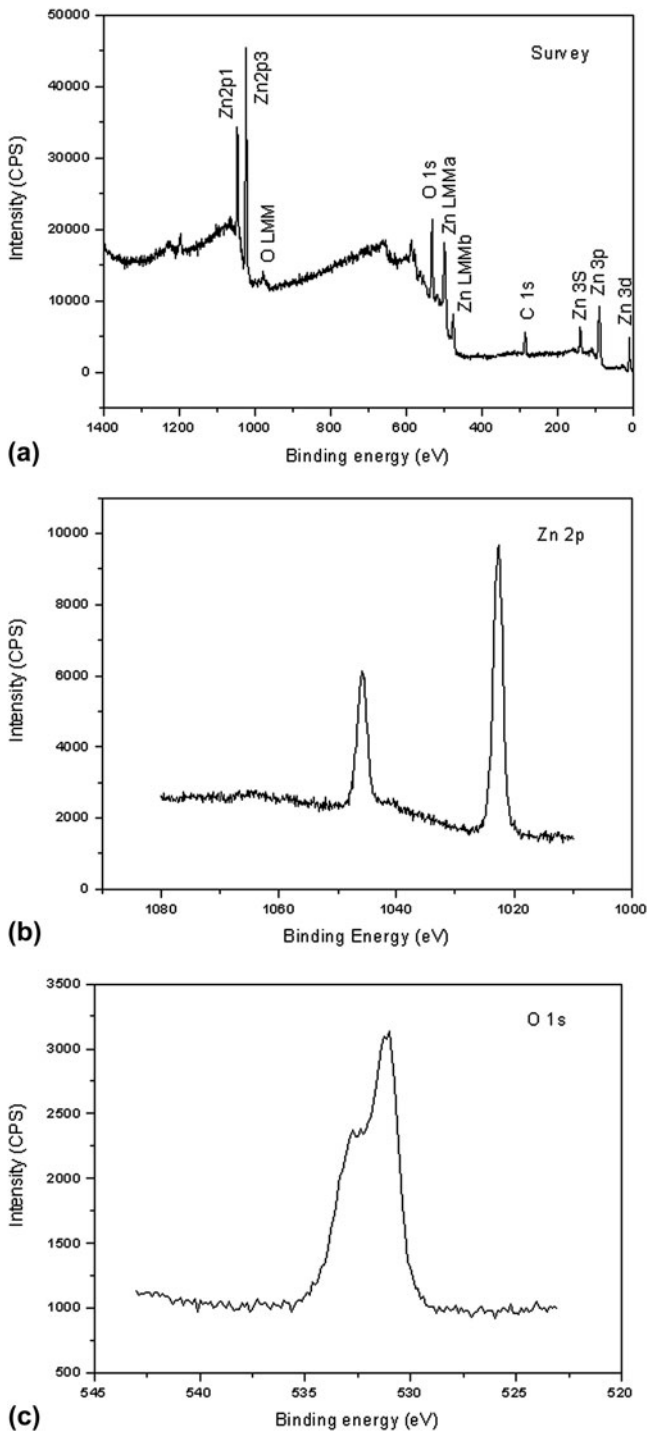


FIG. 2. XPS spectra of as-prepared samples. (a) Survey spectrum. (b) and (c) Zn 2p and O 1s core levels, respectively.

completely disappeared after 45 min, as shown in Fig. 5. The decrease in C–H vibrational bands indicates that the stearic acid is gradually photodegraded by the ZnO hierarchical micro/nanostructures under UV irradiation.

Usually, surface wettability is related to roughness of the material surface. Two models are established to describe the water dewetting behavior on rough films. When a water

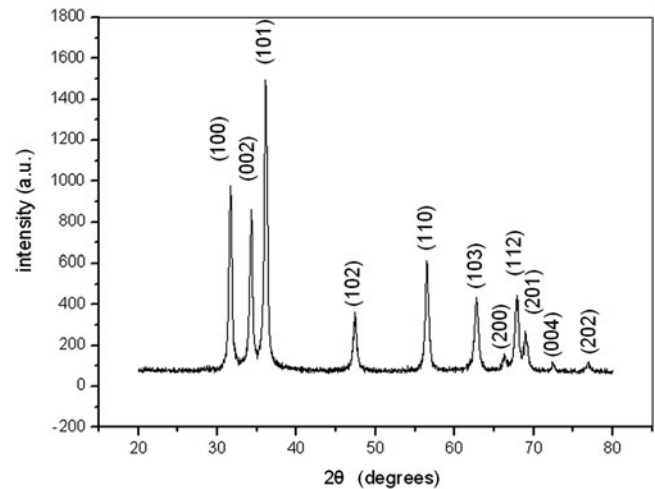


FIG. 3. XRD pattern of the sample shown in Fig. 1(a).

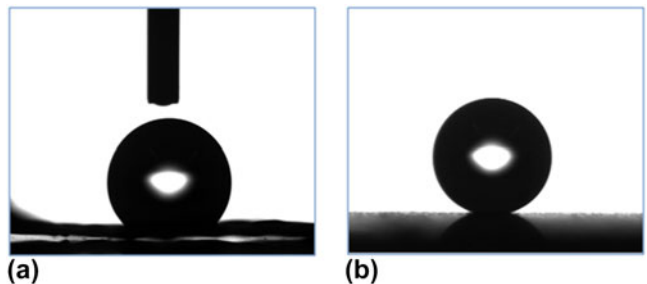


FIG. 4. Water CA of ZnO hierarchical micro/nanostructures. (a) and (b) Water CA before and after chemical modification with low free energy materials. Water CA: (a) 138° and (b) 168°.

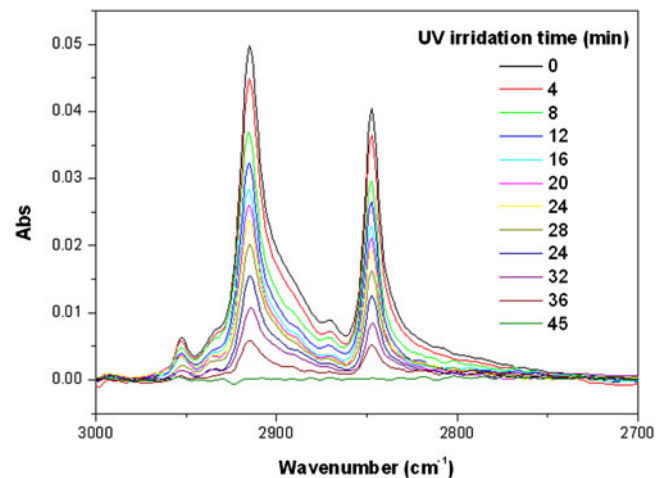


FIG. 5. Photocatalytic activity of ZnO hierarchical micro/nanostructured film by monitoring the photodegradation of stearic acid.

droplet can dip into the pore or grooves on material surfaces, Wenzel described this case as follows<sup>46,47</sup>:

$$\cos \theta_r = r \cos \theta \quad , \quad (1)$$

where  $r$  is the roughness factor, which is the ratio of the total surface area to the projected area on the horizontal plane, and  $\theta_r$  and  $\theta$  are the CAs on a rough film and a native film with smooth surface, respectively. For a Wenzel type surface, obviously, increasing roughness can enhance both hydrophobicity of the hydrophobic surface and hydrophilicity of the hydrophilic surface. The water CA ( $\theta$ ) of the relative flat ZnO film is  $109^\circ$ , as previously reported. Obviously, the roughness of such hierarchical micro/nanostructured films is much increased, therefore, the water CA will be further enhanced according to Eq. (1) and corresponding value is  $138^\circ$ . According to Eq. (1), the roughness ( $r$ ) of hierarchical ZnO micro/nanostructured materials can be estimated to be 2.28. This rough surface is very helpful to adsorb organic molecules on it for further photocatalytic degradation.

When a small water droplet is added on the hierarchical micro/nanostructured film chemically modified with low free energy materials, air can be trapped in interstices, grooves, or corrugations that are produced among microstructures or between the microstructure and the nanostructure. In this case, another model presented by Cassie and Baxter<sup>48</sup> can be generally used as follows:

$$\cos\theta_r = f_1 \cos\theta - f_2 \quad , \quad (2)$$

where  $f_1$  is the contact area fraction with the hierarchical micro/nanostructure and  $f_2 = 1 - f_1$  is that with air trapped by interstices or grooves in the films in the contact area of a water droplet with the film surface. Evidently, increasing  $f_2$  can lead to larger  $\theta_r$ ; that is, the area fraction on the surface trapped air is important to the superhydrophobicity for Cassie and Baxter's type surface. Since the measured water CAs of the flat ZnO surface and the ZnO hierarchical micro/nanostructured film modified with fluoroalkylsilane are  $109^\circ$  and  $168^\circ$ , respectively,  $f_2$  for the as-prepared surface was calculated to be 0.97. This very high value of  $f_2$  reveals that the hierarchical micro/nanostructured film possesses an excellent ability to trap a large amount of air between the microstructure and the nanostructure and that the strong superhydrophobicity with a self-cleaning effect of the hierarchical surface mainly originates from the unique hierarchical micro/nanostructures and the subsequent surface chemical modification. Generally, ZnO can be used to fabricate different films with rough surfaces, i.e., nanorod or nanowire film by solution growth,<sup>49</sup> porous films by electrodeposition,<sup>50</sup> periodic pore arrays by template route,<sup>51</sup> etc. which demonstrate superhydrophobicity after chemical modification. However, our method is relatively facile, and the superhydrophobicity is much better than these reported methods.

ZnO, as a wide band gap semiconductor, possesses many technological applications and has been widely investigated. For example, it can be used as photocatalysts to decompose organic pollutants under visible or UV light

irradiation. Cui et al.<sup>52</sup> revealed the photocatalytic reduction performance of nanostructured ZnO and showed that the photoexcited electrons from ZnO by visible light irradiation can transform  $\text{CO}_2$  into other organic molecules of HCOOH,  $\text{CH}_3\text{OH}$ , and HCHO. Zhou et al.<sup>53</sup> found that tetrapod-like ZnO nanowhiskers demonstrated a better photodegradation to methyl-orange than nanostructured  $\text{TiO}_2$ . Herein, we revealed that such ZnO hierarchical micro/nanostructured films displayed a very good photocatalytic activity to stearic acid. Generally, the crystal phase, crystal composition, material microstructures, adsorption ability to organic molecules, and the specific surface area significantly affect the photocatalytic properties of ZnO. In our case, the ZnO hierarchical micro/nanostructured film has porous structures, rough surface, and possesses a much higher specific surface area and better adsorption ability to stearic acid than that of a flat ZnO film, which contribute to excellent photocatalytic properties. Compared with recent results of photocatalytic

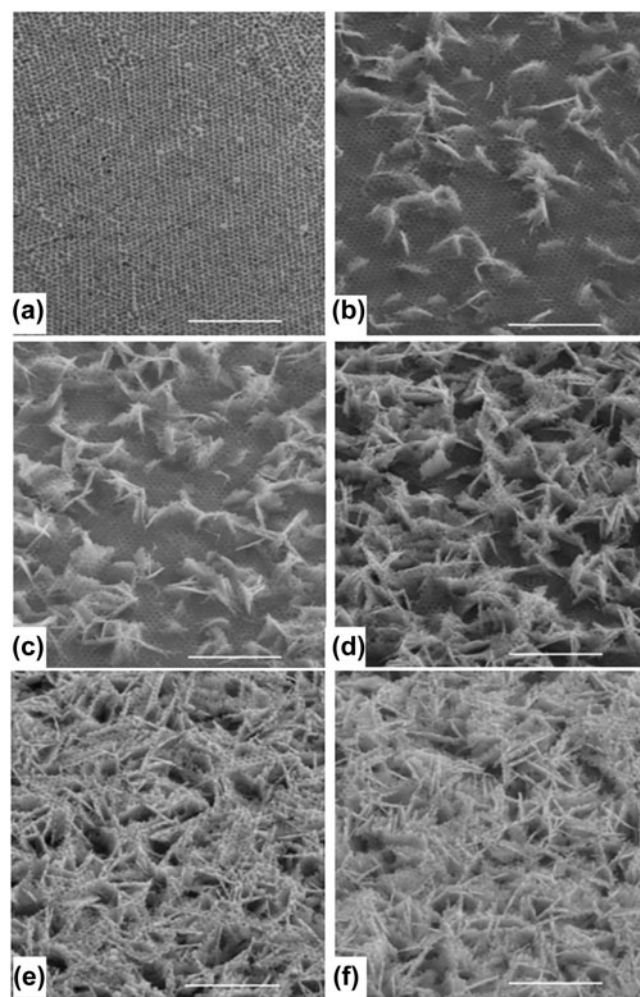


FIG. 6. Morphology evolution of samples at various precursor concentrations. Zinc nitrate concentration: (a) 0.3 M, (b) 0.4 M, (c) 0.5 M, (d) 0.6 M, (e) 0.7 M, and (f) 0.8 M. PS sphere size in colloidal monolayer: 350 nm. Scale bars: 5  $\mu\text{m}$ .

activity of ZnO nanostructures,<sup>54–56</sup> i.e., nanoparticles, nanowires, nanotubes by UV light, our ZnO hierarchical micro/nano-structures showed much lower photo-degradation time, possessing a better photocatalytic performance.

The formation mechanism of such ZnO hierarchical micro/nanostructured materials was investigated by observing the morphology evolution of samples using different precursor concentrations. The periodic nanohole array [Fig. 6(a)] was achieved at very low precursor concentration, to say, 0.3 M, these hole size agrees with PS sphere size in the colloidal monolayer, indicating that these holes were templated from the colloidal monolayer, as previously reported.<sup>52</sup> With increase of precursor concentration, some microsized plates begin to grow with tilted angle from 0 to 90° on the hole array films and some nanoholes formed from colloidal spheres existed on microplate surfaces [Fig. 6(b)]. With further increase of precursor concentration, the number density of microplate with nanoholes also increased, as displayed from Figs. 6(b)–6(f). At very high concentration, the microplates with nanoholes distributed over all the substrate, as shown in Figs. 6(e) and 6(f). As we know, at low precursor concentrations, the mass of ZnO is low after decomposition of precursor by annealing. The growth of ZnO crystals will be completely restricted in the interstices of the colloidal monolayer template, and ZnO periodic hole array is formed after removal of template by annealing, as displayed in Fig. 7(c). With increase of precursor concentration, the mass of ZnO also increases. In this case, the colloidal monolayer cannot absolutely confine the growth of ZnO, the growth of ZnO gradually dominates, and some microplates of ZnO are formed breaking through the limitation of the colloidal template.<sup>57,58</sup> The ZnO microplate can be easily formed under

moderate conditions, as widely reported. However, a periodic hole array is still partially produced on the uphill surface of ZnO microplate due to the effect of the colloidal monolayer, as demonstrated in Fig. 7(c). With further increase of precursor concentration, the mass of ZnO also further increases and the number density of ZnO microplate becomes larger. This high number density of ZnO microplate will produce large surface area and high surface roughness, further resulting in the enhanced photocatalytic activity and superhydrophobicity with self-cleaning on such hierarchical micro/nanostructure surfaces. These hierarchical ZnO micro/nanostructured materials might have important applications in environmental science, microfluidic devices, etc.

#### IV. CONCLUSIONS

A route has been developed to prepare hierarchical ZnO microplate/nanohole-structured materials using a colloidal monolayer as the template by the precursor thermal decomposition. The investigation of the formation mechanism indicated that such special hierarchical structures were formed by both incompletely restricted ZnO growth of colloidal templates and preferable growth of microplates induced by high precursor concentration. With increase of precursor concentration, the number density of ZnO microplates tends to be larger. The large number density of ZnO microplates and holes on the microplates render the sample a large surface area and surface roughness, which is attributed to enhanced photocatalytic activity and superhydrophobicity with self-cleaning effect of such hierarchical micro/nanostructured materials.

#### ACKNOWLEDGMENTS

This work was financially supported by the Natural Science Foundation of China (Grant Nos. 50831005 and 10974203), Recruitment Program of Global Experts (C), and Anhui Provincial Natural Science Foundation for Distinguished Young Scholar (Grant No. 1108085J20).

#### REFERENCES

1. R. Yan, D. Gargas, and P. Yang: Nanowire photonics. *Nat. Photonics* **3**, 569 (2009).
2. E. Roduner: Size matters: Why nanomaterials are different. *Chem. Soc. Rev.* **35**, 583 (2006).
3. C.M. Cobley, J. Chen, E.C. Cho, L.V. Wang, and Y. Xia: Gold nanostructures: A class of multifunctional materials for biomedical applications. *Chem. Soc. Rev.* **40**, 44 (2011).
4. Z.L. Wang: Towards self-powered nanosystems: From nanogenerators to nanopiezotronics. *Adv. Funct. Mater.* **18**, 3553 (2008).
5. R.A. Varin, L. Zbironiec, M. Polanski, and J. Bystrzycki: A review of recent advances on the effects of microstructural refinement and nano-catalytic additives on the hydrogen storage properties of metal and complex hydrides. *Energies* **4**, 1 (2011).
6. M. Morariu, N. Voicu, E. Schäffer, Z. Lin, T.P. Russell, and U. Steiner: Hierarchical structure formation and pattern replication induced by an electric field. *Nat. Mater.* **2**, 48 (2003).

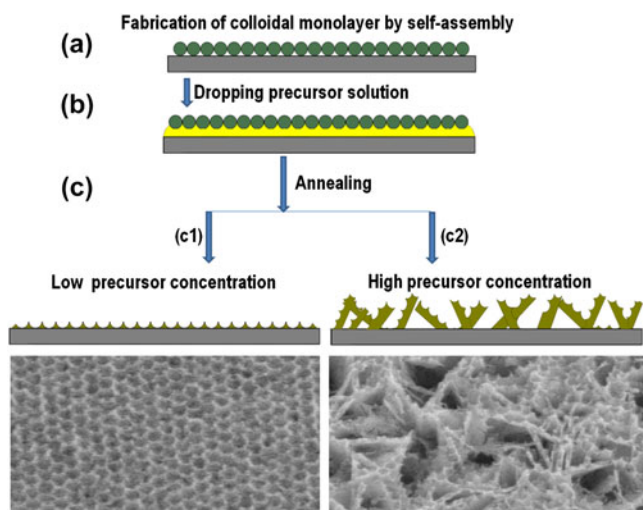


FIG. 7. Formation process of ZnO hierarchical microplate/nanohole structured materials. (a) Fabrication of colloidal monolayer by self-assembly, (b) applying the precursor solution on the colloidal template, (c) annealing the samples at 400 °C for 3 h.

7. S.V. Dorozhkin: A hierarchical structure for apatite crystals. *J. Mater. Sci. - Mater. Med.* **18**, 363 (2007).
8. G. Duan, W. Cai, Y. Luo, Y. Li, and Y. Lei: Hierarchical surface rough ordered Au particle arrays and their surface enhanced Raman scattering. *Appl. Phys. Lett.* **89**, 181918 (2006).
9. J.Y. Lao, J.G. Wen, D.Z. Wang, and Z.F. Ren: Hierarchical ZnO nanostructures. *Nano. Lett.* **2**, 1287 (2002).
10. P.X. Gao, Y. Ding, and Z.L. Wang: Crystallographic-orientation aligned ZnO nanorods grown by tin catalyst. *Nano. Lett.* **3**, 1315 (2003).
11. S.O. Cho, E.J. Lee, H.M. Lee, J.G. Kim, and Y.J. Kim: Controlled synthesis of abundantly branched, hierarchical nanotrees by electron irradiation of polymers. *Adv. Mater.* **18**, 60 (2006).
12. L. Wang, S.J. Guo, and S.J. Dong: Facile electrochemical route to directly fabricate hierarchical spherical cupreous micro structures: Toward superhydrophobic surface. *Electrochem. Commun.* **10**, 655 (2008).
13. C. Wu, L. Lei, X. Zhu, J. Yang, and Y. Xie: Large-Scale synthesis of titanate and anatase tubular hierarchitectures. *Small Mol.* **3**, 1518 (2007).
14. Y. Li, T. Sasaki, Y. Shimizu, and N. Koshizaki: Hexagonal-close-packed, hierarchical amorphous TiO<sub>2</sub> nanocolumn arrays: Transferability, enhanced photocatalytic activity, and superamphiphilicity without UV irradiation. *J. Am. Chem. Soc.* **130**, 14755 (2008).
15. Y. Li, T. Sasaki, Y. Shimizu, and N. Koshizaki: A hierarchically ordered TiO<sub>2</sub> hemispherical particle array with hexagonal-non-close-packed tops: Synthesis and stable superhydrophobicity without UV irradiation. *Small Mol.* **4**, 2286 (2008).
16. W. Barthlott and C. Neinhuis: Purity of the sacred lotus, or escape from contamination in biological surfaces. *Planta Med.* **202**, 1 (1997).
17. T.L. Sun, L. Feng, X.F. Gao, and L. Jiang: Bioinspired surfaces with special wettability. *Acc. Chem. Res.* **38**, 644 (2005).
18. S.T. Wang, Y.L. Song, and L. Jiang: Photoresponsive surfaces with controllable wettability. *J. Photochem. Photobiol., C* **8**, 18 (2007).
19. X-M. Li, D. Reinhoudt, and M. Crego-Calama: What do we need for a superhydrophobic surface? A review on the recent progress in the preparation of superhydrophobic surfaces. *Chem. Soc. Rev.* **36**, 1350 (2007).
20. N.J. Shirtcliffe, G. McHale, S. Atherton, and M.I. Newton: Introduction to superhydrophobicity. *Adv. Colloid Interface Sci.* **161**, 124 (2010).
21. A. Nakajima, K. Hashimoto, and T. Watanabe: Recent studies on super-hydrophobic films. *Monatsh. Chem.* **132**, 31 (2001).
22. Z. Guo, W. Liu, and B-L. Su: Superhydrophobic surfaces: From natural to biomimetic to functional. *J. Colloid Interface Sci.* **353**, 335 (2011).
23. W. Chen, A. Fadeev, M. Hsieh, D. Öner, J. Youngblood, and T. McCarthy: Ultrahydrophobic and ultralyophobic surfaces: Some comments and examples. *Langmuir* **15**, 3395 (1999).
24. J.T. Han, S.Y. Kim, J.S. Woo, and G-W. Lee: Transparent, conductive, and superhydrophobic films from stabilized carbon nanotube/silane sol mixture solution. *Adv. Mater.* **20**, 3724 (2008).
25. K.K.S. Lau, J. Bico, K.K.B. Teo, M. Chhowalla, G.A.J. Amaratunga, W.I. Milne, G.H. McKinley, and K.K. Gleason: Superhydrophobic carbon nanotube forests. *Nano. Lett.* **3**, 1701–1705 (2003).
26. G. Zhang, D.Y. Wang, Z-Z. Gu, and H. Möhwald: Facile fabrication of super-hydrophobic surfaces from binary colloidal assembly. *Langmuir* **21**, 9143 (2005).
27. A. Nakajima, A. Fujishima, K. Hashimoto, and T. Watanabe: Superhydrophobic films from raspberry-like particles. *Adv. Mater.* **11**, 1365 (1999).
28. L. Zhang, Z. Zhou, B. Cheng, J.M. DeSimone, and E.T. Samulski: Superhydrophobic behavior of a perfluoropolyether lotus-leaf-like topography. *Langmuir* **22**, 8576 (2006).
29. F. Xia, L. Feng, S. Wang, T. Sun, W. Song, W. Jiang, and L. Jiang: Dual-responsive surfaces that switch between superhydrophilicity and superhydrophobicity. *Adv. Mater.* **18**, 432 (2006).
30. S. Wang, L. Feng, and L. Jiang: One-step solution-immersing process towards bionic superhydrophobic surfaces. *Adv. Mater.* **18**, 767 (2006).
31. E.J. Lee, H.M. Lee, Y. Li, L.Y. Hong, D.P. Kim, and S.O. Cho: Hierarchical pore structures fabricated by electron irradiation of silicone grease and their applications to superhydrophobic and superhydrophilic films. *Macromol. Rapid Commun.* **28**, 246 (2007).
32. Y. Li, W.P. Cai, B.Q. Cao, G.T. Duan, F.Q. Sun, C.C. Li, and L.C. Jia: Two-dimensional hierarchical porous silica film and its tunable superhydrophobicity. *Nanotechnology* **17**, 238 (2006).
33. Y. Li, G.T. Duan, and W.P. Cai: Controllable superhydrophobic and lipophobic properties of ordered pore indium oxide array films. *J. Colloid Interface Sci.* **314**, 615 (2007).
34. G. Zhang and D. Wang: Colloidal lithography—the art of nano-chemical patterning. *Chem. Asian J.* **4**, 236 (2009).
35. Y. Li, N. Koshizaki, and W. Cai: Periodic one-dimensional nano-structured arrays based on colloidal templates, applications, and devices. *Coord. Chem. Rev.* **255**, 357 (2011).
36. Y. Li, W. Cai, and G. Duan: Ordered micro/nanostructured arrays based on the monolayer colloidal crystals. *Chem. Mater.* **20**, 615 (2008).
37. Y. Li, W.P. Cai, B.Q. Cao, G.T. Duan, C.C. Li, F.Q. Sun, and H.B. Zeng: Morphology-controlled 2D ordered arrays by heating-induced deformation of 2D colloidal monolayer. *J. Mater. Chem.* **16**, 609 (2006).
38. G.T. Duan, W.P. Cai, Y. Li, Z.G. Li, B.Q. Cao, and Y.Y. Luo: Transferable ordered Ni hollow sphere arrays induced by electro-deposition on colloidal monolayer. *J. Phys. Chem. B* **110**, 7184 (2006).
39. Y. Li, C.C. Li, S.O. Cho, G.T. Duan, and W.P. Cai: Silver hierarchical bowl-like array: Synthesis, superhydrophobicity, and optical properties. *Langmuir* **23**, 9802 (2007).
40. Y. Li, X.J. Huang, S.H. Heo, C.C. Li, Y.K. Choi, W.P. Cai, and S.O. Cho: Superhydrophobic bionic surfaces with hierarchical microsphere/SWCNT composite arrays. *Langmuir* **23**, 2169 (2007).
41. Y. Li, E.J. Lee, and S.O. Cho: Superhydrophobic coatings on curved surfaces featuring remarkable supporting force. *J. Phys. Chem. C* **111**, 14813 (2007).
42. W-L. Min, B. Jiang, and P. Jiang: Bioinspired self-cleaning anti-reflection coatings. *Adv. Mater.* **20**, 3914 (2008).
43. A. Kosiorek, W. Kandulski, H. Glaczynska, and M. Giersig: Fabrication of nanoscale rings, dots, and rods by combining shadow nanosphere lithography and annealed polystyrene nanosphere masks. *Small Mol.* **1**, 439 (2005).
44. K.X. Wang, B.D. Yao, M.A. Morris, and J.D. Holmes: Supercritical fluid processing of thermally stable mesoporous titania thin films with enhanced photocatalytic activity. *Chem. Mater.* **17**, 4825 (2005).
45. X.T. Zhang, M. Jin, Z.Y. Liu, D.A. Tryk, S. Nishimoto, T. Murakami, and A. Fujishima: Superhydrophobic TiO<sub>2</sub> surfaces: Preparation, photocatalytic wettability conversion, and superhydrophobic-superhydrophilic patterning. *J. Phys. Chem. C* **111**, 14521 (2007).
46. W. Gao, L. Dickinson, C. Grozinger, F.G. Morin, and L. Reven: Self-assembled monolayers of alkylphosphonic acids on metal oxides. *Langmuir* **12**, 6429 (1996).
47. R.N. Wenzel: Surface roughness and contact angle. *J. Phys. Colloid Chem.* **53**, 1446 (1949).
48. A.B.D. Cassie and S. Baxter: Wettability of porous surfaces. *Trans. Faraday Soc.* **40**, 546 (1944).

49. G. Kwak, M. Seol, Y. Tak, and K. Yong: Superhydrophobic ZnO nanowire surface: Chemical modification and effects of UV irradiation. *J. Phys. Chem. C* **113**, 12085 (2009).
50. M. Li, J. Zhai, H. Liu, Y. Song, L. Jiang, and D. Zhu: Electrochemical deposition of conductive superhydrophobic zinc oxide thin films. *J. Phys. Chem. B* **107**, 9954 (2003).
51. Y. Li, W.P. Cai, G.T. Duan, B.Q. Cao, F.Q. Sun, and F. Lu: Superhydrophobicity of 2D ZnO ordered pore arrays formed by solution-dipping template method. *J. Colloid Interface Sci.* **287**, 634 (2005).
52. J.J. Cui, Q.H. Yang, and X.D. Wang: Photocatalysed reduction nature of nano ZnO. *Bull. Chin. Ceram. Soc.* **1**, 23 (2006).
53. J.P. Zhou, W.L. Fu, K.Q. Qiu, and Q.Y. Chen: Wettability of porous two dimensional ZnO nanocrystal films. *J. Funct. Mater. Dev.* **13**, 195 (2007).
54. H. Liu, B. Huang, X. Qin, X. Zhang, and Z. Wang: Fabrication and photocatalytic of mushroom-like ZnO microcrystals via a solvothermal route. *Rare Met.* **30**, 173 (2011).
55. C. Ma, Z. Zhou, H. Wei, Z. Yang, Z. Wang, and Y. Zhang: Rapid large-scale preparation of ZnO nanowire for photocatalytic application. *Nano. Res. Lett.* **6**, 536 (2011).
56. M. Nasr-Esfahani and A. Nekoubin: Well-aligned arrays of vertically oriented ZnO nanorod films for photocatalytic degradation of textile dye. *AIP Conf. Proc.* **1341**, 309 (2011).
57. F. Sun, W. Cai, Y. Li, B. Cao, Y. Lei, and L. Zhang: Morphology-controlled growth of large-area two-dimensional ordered pore arrays. *Adv. Funct. Mater.* **14**, 283 (2004).
58. Y. Li, W. Cai, G. Duan, B. Cao, and F. Sun: Two-dimensional ordered polymer hollow sphere and convex structure arrays based on monolayer pore films. *J. Mater. Res.* **20**, 338 (2005).